Plastic bending and shape-memory effect of double-wall carbon nanotubes

Hideki Mori,[1] Shigenobu Ogata,[1] Ju Li,[2] Seiji Akita,[3] and Yoshikazu Nakayama[4,*]
[1]*Department of Mechanical Science and Bioengineering, Osaka University, Osaka 560-8531, Japan*
[2]*Department of Materials Science and Engineering, Ohio State University, Columbus, Ohio 43210, USA*
[3]*Department of Physics and Electronics, Osaka Prefecture University, Osaka 599-8531, Japan*
[4]*Department of Mechanical Engineering, Osaka University, Osaka 565-0871, Japan*
(Received 30 March 2007; published 3 October 2007)

Plastic bending of (5,5)@(10,10) double-wall carbon nanotube is analyzed using nudged elastic band minimum energy path calculations. At lower applied bending curvature, only the outer tube deforms plastically. However, at higher bending curvature, both the inner and outer tubes deform plastically. We find that the plastic deformation of the outer tube is more difficult than that of isolated single-wall carbon nanotube of the same diameter due to tube-tube interactions. In contrast, the plastic deformation of the inner tube is not strongly affected by the presence of the outer tube. We also analyze the shape-memory effect (SME) discovered experimentally, which is a thermal recovery process from the plastically bent state to the straight defect-free state, which can be repeated multiple times. We analyze the physics behind SME of carbon nanotubes, which is quite different from that of traditional shape-memory alloys.

DOI: 10.1103/PhysRevB.76.165405 PACS number(s): 62.20.Fe, 81.07.De, 62.25.+g, 81.05.Zx

I. INTRODUCTION

Processing and manipulation of carbon nanotubes (CNTs) such as handling,[1–3] welding,[4,5] machining,[6,7] and deformation[8] are vital for their adoption in nanoscale devices. Recently, Nakayama *et al.* succeeded in *in situ* observation of the plastic bending of double-wall carbon nanotubes (DWNTs) in transmission electron microscope.[9] They used Pt-coated scanning probe microscope tip to induce bending and simultaneously passed electrical current through the CNT. The DWNT is resistively heated to a temperature exceeding 1000 K, and upon withdrawal of both the current and the bending force, the tube is found to be plastically bent. This does not occur if there is no current. Furthermore, they observed the curing or thermal recovery phenomenon of the plastically bent carbon nanotube.[10] For additional current induced, the plastically bent DWNT returns to the original straight form. The DWNT can repeatedly cycle between the plastically bent and elastic straight states.

The above phenomenon qualifies as one-way shape-memory effect (SME),[11,12] which has been observed in macroscopic crystalline materials[13,14] and polymers.[15] Shape-memory effect has found application in a variety of devices such as sensors and actuators,[12] stents,[16] and artificial tissues.[17] With SME discovered in carbon nanotubes,[10] it is conceivable that one could build nanoscaffolds using straight or elastically bent CNTs and plastically bend the scaffold arbitrarily at certain temperature T_1, which upon heating to another temperature T_2 recovers the original scaffold shape composed of straight or elastically bent CNTs.

The plastic deformation of carbon nanotubes is accomplished by the nucleation and motion of dislocations, same as three-dimensional (3D) bulk crystals.[18–20] However, there are some important differences in the dislocation dynamics of quasi-one-dimensional nanotubes compared to 3D crystals. One is the lack of the Frank-Read source.[21] Since dislocations in nanotubes are not line defects, the usual ways of dislocation multiplication by double cross slip and other Frank-Read-type processes are denied to the nanotubes. Therefore, nucleation of dislocations tends to be an important issue in the plastic deformation of CNT.[18–20] The other is the lack of dislocation sinks such as free surfaces or grain boundaries (except at the nanotube terminations), as well as dislocation entangling mechanisms. Because of this, perhaps most dislocations in nanotubes are geometrically necessary dislocations (GNDs),[22] since it appears difficult to stabilize statistically stored dislocations without extensive entangling. The number of variety of dislocations in nanotubes is much smaller than in 3D crystals. The lack of dislocation reaction, entangling, and sink mechanisms means that irreversibility of the plastic deformation is not enforced as in bulk crystals, which we believe is the main reason behind the experimentally observed shape-memory effect of CNTs.

On a perfect nanotube, the dislocations must be nucleated in pairs, the smallest embryo which is the so-called 5-7-7-5 (Stone-Wales) defect.[23] It can be formed by 90° rotation of a single bond in the graphene plane, which transforms four adjacent hexagons into two pentagons and two heptagons. This 5-7-7-5 defect can then dissociate into a 5-7 defect (+ dislocation) and a 7-5 defect (− dislocation) by successive 90° rotation of neighboring C-C bonds.[18] Successive reverse rotations of the C-C bonds in a plastically bent CNT cause the CNT to become perfect again. In a previous report,[24] we have investigated the energetics of plastic bending of single-wall carbon nanotubes (SWNTs) using minimum energy path atomistic calculation[25,26] with a bond-order potential.[27] We have determined the temperature and mechanical conditions to accomplish plastic bending of SWNTs and have found that, for instance, the SWNT must sustain significant elastic bending before it becomes thermodynamically favorable to bend plastically.[24]

Because our experimental systems are double-wall carbon nanotubes,[10] layer interactions must be taken into account. This paper investigates defect nucleation and migration pathways in the plastic bending (at finite external stress) and thermal recovery (at zero stress) of a DWNT, building upon previous theoretical work.[18–20,24,28–38]

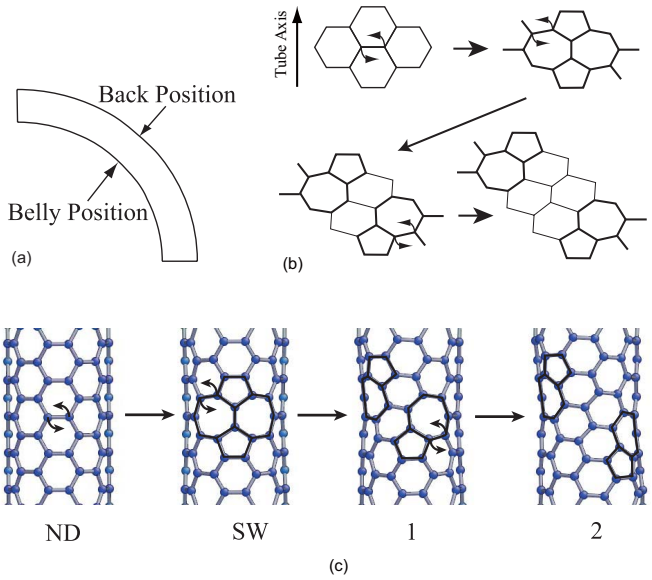

FIG. 1. (Color online) (a) The back and belly positions of a bent CNT, (b) plastic deformation accomplished by bond rotation (adapted from Ref. 18), and (c) plastic deformation accomplished by bond rotation, first nucleation event in (5,5) armchair SWNT. Labels "ND" and "SW" mean the defect-free state and the state with the 5-7-7-5 defect, respectively; the numeral labels are the split step of the 5-7 (+ dislocation) and 7-5 (− dislocation) defect pairs.

II. PLASTIC BENDING MODEL AND NUMERICAL METHOD

To investigate the effect of layer interactions, we focus on one DWNT whose inner tube is (5,5) armchair and outer tube is (10,10) armchair type. We call this (5,5)@(10,10) DWNT. The diameter of the inner tube is D_{inner}=0.68 nm and that of the outer tube is D_{outer}=1.37 nm. Therefore, the interlayer spacing is about 0.34 nm, which is nearly equal to the interlayer spacing of graphite. The tube length in the calculation is 7.4 nm, containing 1800 atoms (600 in inner tube and 1200 in outer tube). We focus only on plastic deformation at the elastically bent state.

To limit our search of the potential energy landscape, we make the following assumptions about the plastic deformation. First, plastic bending is driven mainly by the in-plane bond rotations. Second, processes generating a square or an octagon are not allowed. Third, atoms are not inserted or removed. For DWNT, we make the additional assumption that the layer interactions are nonbonding, weak van der Waals type.[8] Even though out-of-plane displacements are allowed during the bond rotations, they are generally quite small[34] that fusion between the inner tube and outer tube will not happen, as two atoms need to get closer than a cutoff distance of 2.6 Å to form a covalent bond, whereas the equilibrium tube-tube distance is 3.4 Å.

In the initial elastically bent state, we refer to the position of the maximum tensile stress as the "back position," and the position of the maximum compressive stress as the "belly position" [see Fig. 1(a)]. Generally speaking, 5-7-7-5 defect nucleation and the migration of split 5-7 pairs will produce local strain fields on top of the imposed strain and will also cause chirality changes.[18,28,29,31] In armchair-type SWNT, the 5-7-7-5 defect is nucleated at the back position and splits into two 5-7 pairs, which attract each other if without the imposed strain. With the imposed bending strain, the pairs glide away toward the belly position, changing the chirality from (n,n) to $(n,n-1)$ in the domain between the two defects. For example, the (5,5) armchair type changes its chirality from (5,5) to (5,4) at the back position. This relaxes the local tensile and compressive strain, respectively [see Fig. 1(b)].

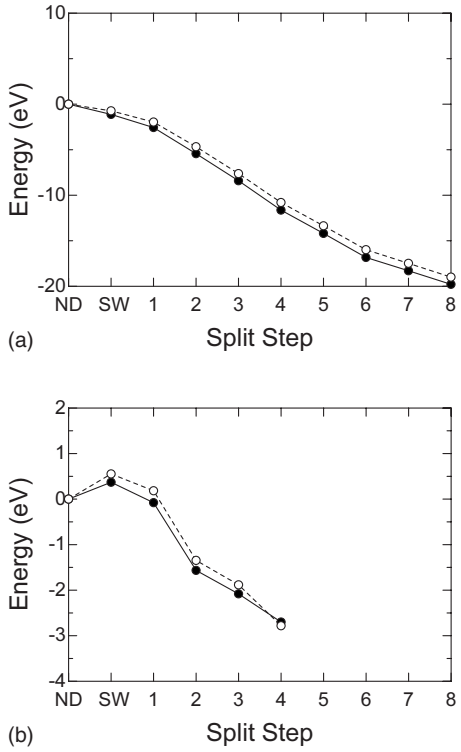

FIG. 2. The effect of boundary condition on the energetics of 5-7-7-5 defect nucleation and 5-7 defect migration in (a) outer tube and (b) inner tube. Filled circle means that all ends are fixed. Open circle means that both ends of the outer tube are fixed; one end of the inner tube is fixed and the other end is free.

The energetics of 5-7-7-5 defect nucleation, dissociation, and 5-7 defect migration are studied using the nudged elastic band (NEB) method,[25] an efficient technique for finding the minimum energy path (MEP) between specified initial state and final state in hyperspace. We use an analytic bond-order potential for carbon-carbon covalent interactions, which produces accurate binding energies for graphite and diamond.[27,39,40] We use the Lennard-Jones potential for interlayer van der Waals interactions in DWNT, with the parameter set proposed in Ref. 41.

In our NEB calculations, force acting on each atom is relaxed to less than 0.05 eV/Å using simulated annealing relaxation. Activation and formation energies of 5-7-7-5 defect in the (5,5) straight SWNT (stress-free, with a length of 7.4 nm) are estimated to be 7.3 and 3.1 eV, respectively. They fit within the range of recent theoretical studies based on density functional theory: 8.6–9.1 eV for the activation energy[30,34,35] and 2.0–4.0 eV for the formation

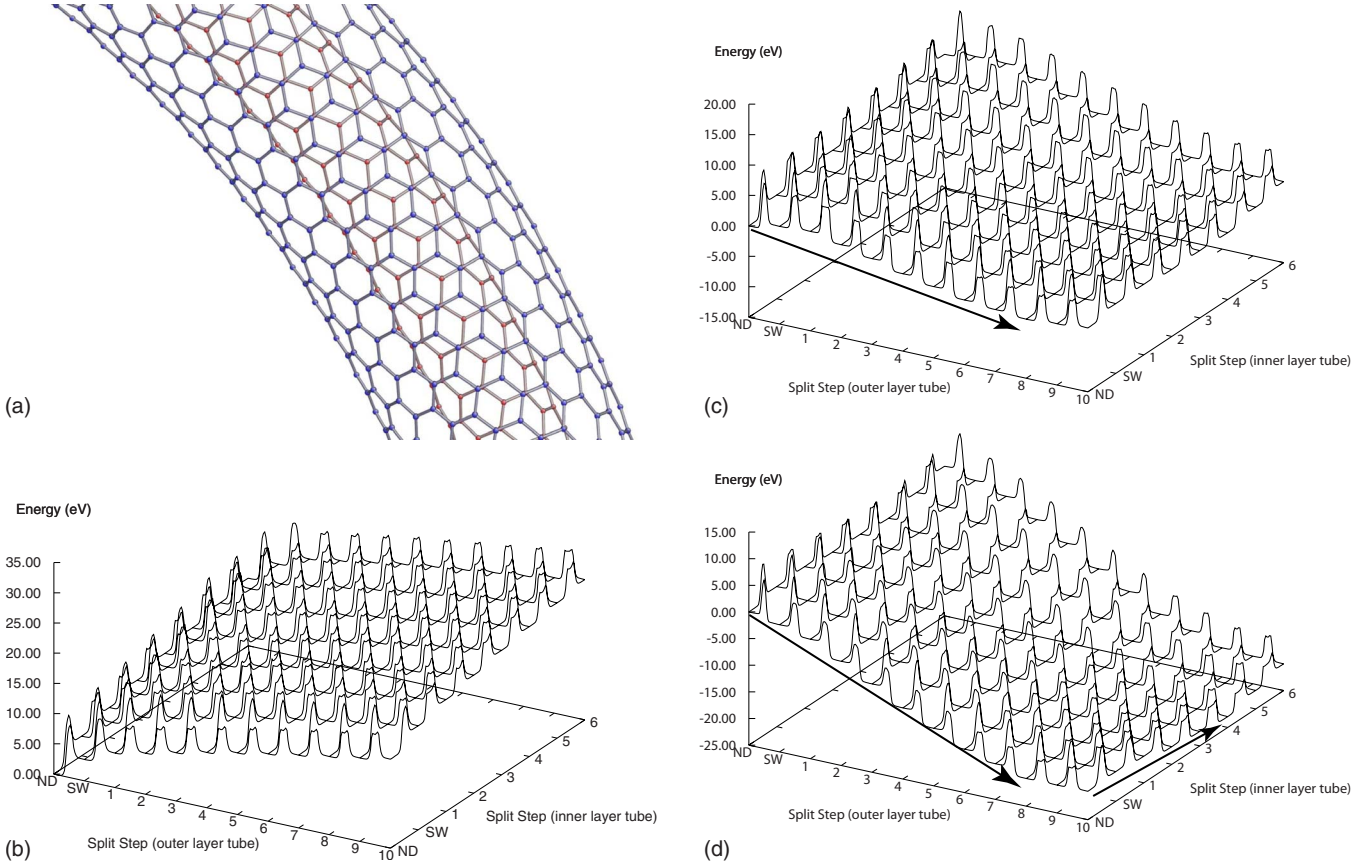

FIG. 3. (Color online) (a) Atomic configuration of an elastically bent (5,5)@(10,10) DWNT at a bending curvature $\rho=0.16$ nm^{-1}. The energetics map of DWNT for 5-7-7-5 defect nucleation and 5-7 pairs migration on (5,5)@(10,10) DWNT at bending curvature (b) $\rho=0$ nm^{-1}, (c) $\rho=0.08$ nm^{-1}, and (d) $\rho=0.16$ nm^{-1}. Labels ND and SW mean the defect-free state and the state with the 5-7-7-5 defect, respectively. x axis and y axis are the split steps of the two pairs of dislocations on the inner and outer tubes, respectively. Arrow shows minimum energy path.

energy.[19,20,30,32–34] The activation and formation energies of 5-7-7-5 defect and the migration path of 5-7 pairs at finite bending curvature ρ are then calculated under fixed-displacement boundary condition at both ends of the outer and inner tubes. One may also fix the outer tube ends while letting one inner tube end free, but the effect of this boundary condition change is less than 1 eV from Figs. 2(a) and 2(b) and does not change the qualitative features of our results.

III. RESULTS

The (5,5)@(10,10) DWNT is shown in Fig. 3(a). We plot the NEB optimized energetics of DWNT at zero and two other bending curvatures in Figs. 3(b)–3(d) as a function of plasticity order parameters—the split step between 5-7 (+ dislocation) and 7-5 (− dislocation) defects on the inner and outer tubes, respectively. For straight and stress-free tube [Fig. 3(b)], the formation energy increases with increasing split steps. Obviously, 5-7-7-5 defect nucleation and pair migrations are thermodynamically unfavorable when there is no external stress. However, Figs. 3(c) and 3(d) show that the DWNT prefers defective condition under large bending. At lower bending curvature $\rho=0.08$ nm^{-1}, the energy increases monotonically with increasing split step on the inner tube. Therefore, the plastic deformation occurs only on the outer tube. At this bending curvature, when the 5-7 pair of outer tube glides eight times, the configuration becomes energetically the most stable. In contrast, at higher bending curvature $\rho=0.16$ nm^{-1}, the formation energy of the 5-7 pair on the inner tube starts to decrease with increasing split step after three split steps have been completed on the outer tube. Therefore, the plastic deformation occurs at both outer and inner tubes. At $\rho=0.16$ nm^{-1}, when the 5-7 pair on the outer tube glides eight times and the 5-7 pair on the inner tube glides four times, the configuration becomes energetically the most stable. The globally optimal 5-7 pair configuration is close to the neutral planes of the bent tubes.

Based on the energetics map above, plastic deformation of DWNT always starts at the outer tube. This is because the outer tube sustains higher tensile strain $\epsilon_{\text{outer}}^{\text{back}} \sim \rho D_{\text{outer}}/2$ at the back position than the inner tube at the same elastic bending curvature. With increasing bending curvature ρ, the activation energy for 5-7-7-5 defect nucleation on the outer tube decreases from 8.7 to 6.6 eV. The activation energies for the 5-7 pair migration are not strongly dependent on the bending curvature ρ. They are 5.0–3.0 eV; the average is 4 eV.

We observe buckling instability of the outer tube at bending curvature $\rho_{\text{buckling}}=0.17$ nm^{-1} for the (5,5)@(10,10)

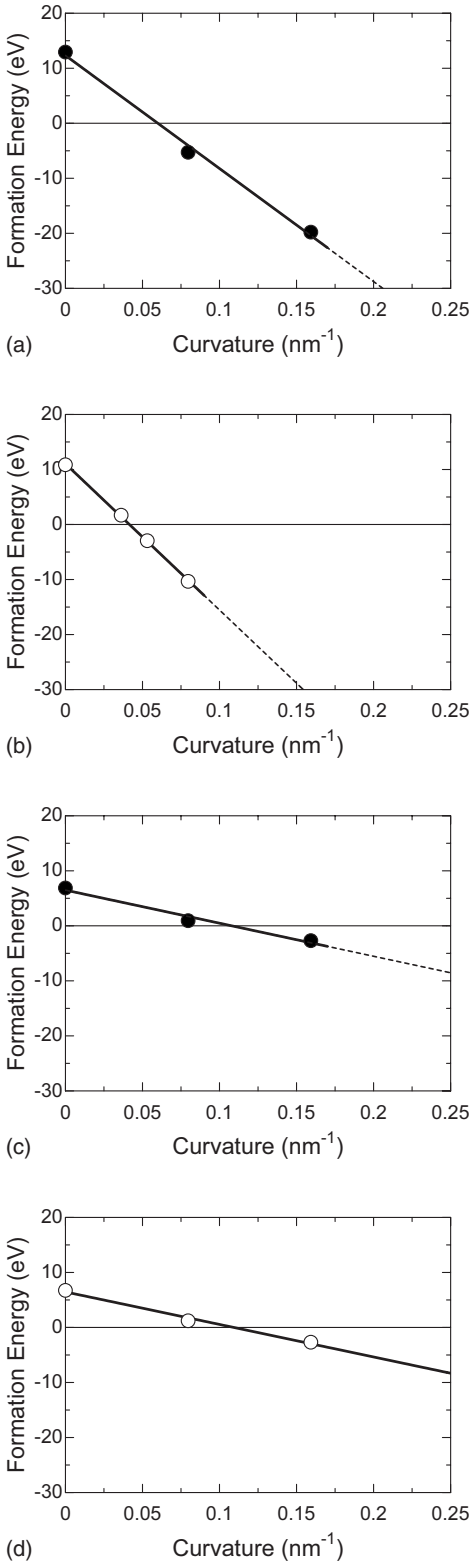

FIG. 4. Formation energies of the defective configuration as a function of the bending curvature ρ in (a) outer tube, (b) (10,10) SWNT, (c) inner tube, and (d) (5,5) SWNT. For the formation energy of the inner tube, we chose the value where the plastic deformation of the outer tube has been completed (after gliding eight times). Solid lines are the linear interpolations. Dashed lines mean the buckling regime.

DWNT, while $\rho_{\text{buckling}}=0.09$ nm^{-1} for (10,10) SWNT. The DWNT is thus more robust against buckling in bending than the SWNT, due to the deformation constraints posed by the existence of the inner tube.

To investigate the thermodynamic (not kinetic) threshold[42] for plastic deformation of the inner and outer tubes, we plot the formation energies of the optimally defective configurations (in reference to the elastically bent state) as a function of bending curvature in Figs. 4(a) and 4(c). The eight (outer) and four (inner) split-step configurations have the minimum potential energy over a wide range of ρ. Therefore, the formation energies of those defects are plotted. For the formation energy of the inner tube, we chose the value where the plastic deformation of the outer tube has been completed (gliding eight times). The formation energy becomes negative at $\rho_{\text{yield}}=0.06$ and 0.11 nm^{-1} for outer tube and inner tubes of DWNT, respectively. These results indicate that the plastically bent state becomes energetically more favorable than the elastically bent state above a "yield curvature" ρ_{yield}. In reference, we also plot the formation energies of the optimally defective (5,5) and (10,10) SWNTs as a function of bending curvature in Figs. 4(b) and 4(d), respectively. The yield curvature of the outer tube is higher than that of (10,10) SWNT ($\rho_{\text{yield}}=0.04$ nm^{-1}), whereas the yield curvature of the inner tube is not greatly different.

The above difference comes from the layer interactions and deformation constraints. During the plastic deformation of the outer tube, the van der Waals potential increases with increasing split step of the outer tube because the interlayer distance becomes shorter as the diameter of the outer tube shrinks. Hence, the plastic deformation of the DWNT outer tube is more difficult than that of SWNT. In contrast, the optimal 5-7 pair formation energy on the inner tube is always almost the same as that of (5,5) SWNT.

Since the highest barrier to plastic deformation in the experimental[9] range of ρ is the activation barrier for 5-7-7-5 defect nucleation, as shown in Fig. 3, we plot the activation barrier for 5-7-7-5 defect nucleation on the outer and inner tubes as a function of bending curvature in Figs. 5(a) and 5(c), respectively. As a reference, we also plot the activation barrier for 5-7-7-5 defect nucleation on (5,5) and (10,10) SWNTs in Figs. 5(b) and 5(d), respectively. Even at $\rho>0.09$ nm^{-1} which is the buckling curvature of (10,10) SWNT, the DWNT does not buckle, while the activation barrier of plastic deformation continues to decrease with increasing ρ, until eventually the activation barrier reaches 6.6 eV at the DWNT buckling curvature of $\rho=0.17$ nm^{-1}. Therefore, athermal nucleation, i.e., zero activation energy condition[43] for the 5-7-7-5 defect nucleation, does *not* occur in DWNT before buckling. The plastic deformation of unbuckled DWNT therefore cannot occur without thermal activation.

Next, we investigate the thermal recovery kinetics from plastically bent tube to nondefective tube at zero stress. We show the energetics map of DWNT and the MEP of SWNT in recovery in Figs. 6(a) and 6(b), respectively. During the calculations, one end of the nanotube is fixed, while the other end is free to move. The defect annihilation energy is negative (in reference to the plastically bent tube) in both SWNT and DWNT. The recovery of SWNT, however, seems to be

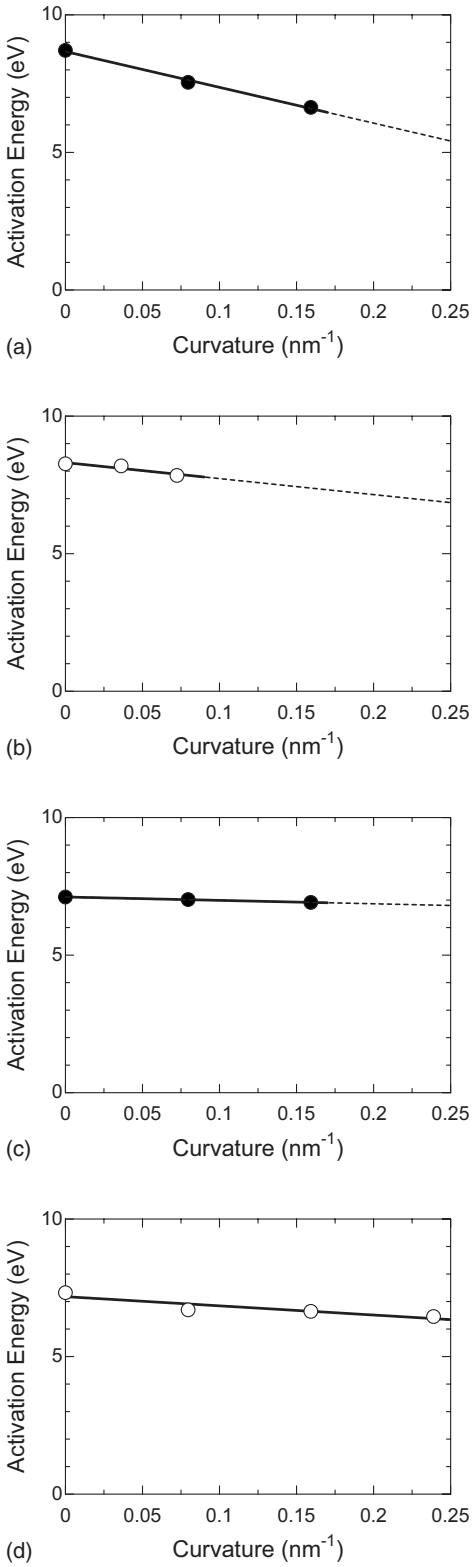

FIG. 5. Activation energies of 5-7-7-5 defect nucleation as a function of the bending curvature ρ in (a) outer tube, (b) (10,10) SWNT, (c) inner tube, and (d) (5,5) SWNT. For the activation energy of the inner tube, we chose the value where the plastic deformation of the outer tube has been completed. Solid line and dashed line are the linear interpolations. Dashed lines mean the buckling regime.

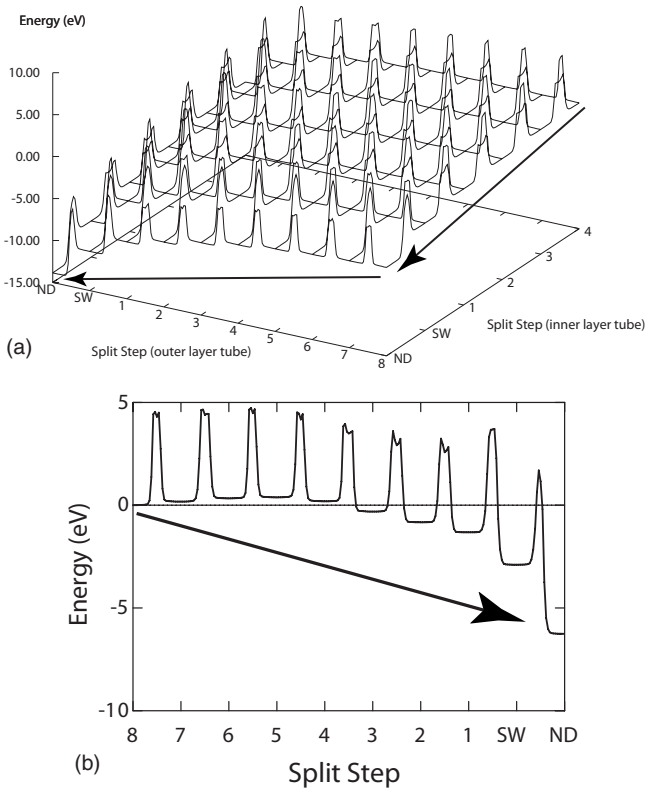

FIG. 6. The NEB optimized recovery energetics of (a) DWNT at zero stress (x axis and y axis are the split step of the 5-7 pair on the inner and outer tubes, respectively) and (b) that of (10,10) SWNT. Labels ND and SW mean the defect-free state and the state with the 5-7-7-5 defect, respectively. The zero-energy point on the map and MEP correspond to the plastically bent state. On the map, it is at $x=8$ and $y=4$. Arrow shows minimum energy path.

more difficult because the 5-7 pair energy increases with decreasing split step during the first several steps [Fig. 6(b)]. In contrast, in DWNT, the 5-7 pair energy decreases monotonically with decreasing split step if the inner tube recovers first, followed by the recovery of the outer tube. Therefore, the thermal recovery of DWNT seems to be kinetically easier than that of SWNT. Quantitatively, the frequency of successful bond rotation depends on the temperature as $\nu \exp(-E_{\mathrm{act}}/k_B T)$, where E_{act} is the activation barrier for 5-7 pair migration and ν is the attempt frequency. Take $T=2000$ K, $\nu=10^{13}$ s^{-1}, and $E_{\mathrm{act}}=5$ eV,[24,34,35] the frequency can be estimated to be 2.5 s^{-1}, and thus the thermal recovery (bond rotations) will occur within a few seconds at $T=2000$ K.

IV. DISCUSSIONS

The plastic bending and shape-memory effect of carbon nanotubes are modeled here by the creation, migration, and annihilation of GNDs.[22] These GNDs are envisioned to be nucleated near the back position of the nanotube, then migrate to optimal "pools" on two sides of the nanotube near the neutral plane of bending.[24] Unlike bending bulk crystals, nanotubes have nanoscale confined geometries; thus, the plastic work done would not compensate for the energy cost

of creating the GNDs if the bending curvature is below certain ρ_{yield}, similar as in the Griffith criterion.[26,42] Motion of the GNDs (90° rotation of C-C bond) incurs large activation barriers, so that the GNDs can be "frozen in" at room temperature, and the nanotube appears plastically bent. However, upon reheating, the GNDs can move back and annihilate, causing the nanotube to recover its straight form. SME happens quite naturally in carbon nanotube because of its unique geometry. The nanoscale confinement means that the GNDs do not travel very far to accomplish the bending, which facilitates the recovery. The lack of dislocation entangling mechanisms means that irreversibility of the plastic deformation is not enforced as in 3D bulk crystals. Similar effect has been observed in nanocrystalline thin films.[44]

We have investigated the role of interlayer interactions (nonbonding) in the plastic bending and thermal recovery of DWNT. At lower bending curvature, only the outer tube prefers defective condition. Then, at higher bending curvature, both the outer and inner tubes prefer defective condition. The plastic deformation as well as buckling of the outer tube are more difficult than that of the same-diameter SWNT due to deformation constraints posed by the inner tube. In this study, we ignored the exchange of atoms between the layers. However, under large elastic deformation and high temperature, this may play an important role in the plastic deformation.[9] Lastly, we note that heating CNTs by electrical current may introduce nonequilibrium physics,[45] which could invalidate the use of simple transition state theory. However the gross features shown in Figs. 3 and 6(a), energy landscapes, reflecting GND core energies, elastic interactions, and plastic work, as well as interlayer interactions, are expected to be robust.

ACKNOWLEDGMENTS

We acknowledge support by the Ministry of Education, Science, Sports and Culture, Grant-in-Aid for Scientific Research on Priority Areas (Grants Nos. 17310084, 17760082, and 17656044) 2006 and Handai Frontier Research Center. Work of J.L. is supported by NSF DMR-0502711, ONR N00014-05-1-0504, AFOSR, DOE, and Ohio Supercomputer Center.

*nakayama@mech.eng.osaka-u.ac.jp

[1] T. Hertel, R. Martel, and P. Avouris, J. Phys. Chem. B **102**, 910 (1998).
[2] J. Plewa, E. Tanner, D. M. Mueth, and D. G. Grier, Opt. Express **12**, 1978 (2004).
[3] H. Nishijima, S. Kamo, S. Akita, Y. Nakayama, K. I. Hohmura, S. H. Yoshimura, and K. Takeyasu, Appl. Phys. Lett. **74**, 4061 (1999).
[4] M. Terrones, F. Banhart, N. Grobert, J. C. Charlier, H. Terrones, and P. M. Ajayan, Phys. Rev. Lett. **89**, 075505 (2002).
[5] I. Jang, S. B. Sinnott, D. Danailov, and P. Keblinski, Nano Lett. **4**, 109 (2004).
[6] M. S. Raghuveer, P. G. Ganesan, J. D'Arcy-Gall, G. Ramanath, M. Marshall, and I. Petrov, Appl. Phys. Lett. **84**, 4484 (2004).
[7] S. Akita, Y. Nakayama, S. Mizooka, Y. Takano, T. Okawa, Y. Miyatake, S. Yamanaka, M. Tsuji, and T. Nosaka, Appl. Phys. Lett. **79**, 1691 (2001).
[8] J. Y. Huang, S. Chen, Z. F. Ren, Z. Q. Wang, D. Z. Wang, M. Vaziri, Z. Suo, G. Chen, and M. S. Dresselhaus, Phys. Rev. Lett. **97**, 075501 (2006).
[9] Y. Nakayama, A. Nagataki, O. Suekane, X. Cai, and S. Akita, Jpn. J. Appl. Phys., Part 2 **44**, L720 (2005).
[10] O. Suekane, A. Nagataki, and Y. Nakayama, Appl. Phys. Lett. **89**, 183110 (2006).
[11] D. Mantovani, JOM **52**, 36 (2000).
[12] K. Otsuka and T. Kakeshita, MRS Bull. **27**, 91 (2002).
[13] K. Otsuka and X. B. Ren, Intermetallics **7**, 511 (1999).
[14] Y. Wang, X. B. Ren, and K. Otsuka, Phys. Rev. Lett. **97**, 225703 (2006).
[15] A. Lendlein and S. Kelch, Angew. Chem., Int. Ed. **41**, 2034 (2002).
[16] T. W. Duerig, MRS Bull. **27**, 101 (2002).
[17] R. Langer and D. A. Tirrell, Nature (London) **428**, 487 (2004).
[18] B. I. Yakobson, Appl. Phys. Lett. **72**, 918 (1998).
[19] P. Zhang, P. E. Lammert, and V. H. Crespi, Phys. Rev. Lett. **81**, 5346 (1998).
[20] M. B. Nardelli, B. I. Yakobson, and J. Bernholc, Phys. Rev. Lett. **81**, 4656 (1998).
[21] F. C. Frank and W. T. Read, Phys. Rev. **79**, 722 (1950).
[22] A. Arsenlis and D. M. Parks, Acta Mater. **47**, 1597 (1999).
[23] A. J. Stone and D. J. Wales, Chem. Phys. Lett. **128**, 501 (1986).
[24] H. Mori, S. Ogata, J. Li, S. Akita, and Y. Nakayama, Phys. Rev. B **74**, 165418 (2006).
[25] G. Henkelman and H. Jonsson, J. Chem. Phys. **113**, 9978 (2000).
[26] T. Zhu, J. Li, and S. Yip, Proc. R. Soc. London, Ser. A **462**, 1741 (2006).
[27] I. I. Oleinik and D. G. Pettifor, Phys. Rev. B **59**, 8500 (1999).
[28] B. I. Dunlap, Phys. Rev. B **46**, 1933 (1992).
[29] L. Chico, V. H. Crespi, L. X. Benedict, S. G. Louie, and M. L. Cohen, Phys. Rev. Lett. **76**, 971 (1996).
[30] Q. Zhao, M. B. Nardelli, and J. Bernholc, Phys. Rev. B **65**, 144105 (2002).
[31] J. Han, M. P. Anantram, R. L. Jaffe, J. Kong, and H. Dai, Phys. Rev. B **57**, 14983 (1998).
[32] P. Jensen, J. Gale, and X. Blase, Phys. Rev. B **66**, 193403 (2002).
[33] Z. Li, P. Dharap, P. Sharma, S. Nagarajaiah, and B. I. Yakobson, J. Appl. Phys. **97**, 074303 (2005).
[34] G. G. Samsonidze, G. G. Samsonidze, and B. I. Yakobson, Phys. Rev. Lett. **88**, 065501 (2002).
[35] T. Dumitrica and B. I. Yakobson, Appl. Phys. Lett. **84**, 2775 (2004).
[36] S. Berber, Y.-K. Kwon, and D. Tomanek, Phys. Rev. Lett. **91**, 165503 (2003).
[37] T. Belytschko, S. P. Xiao, G. C. Schatz, and R. S. Ruoff, Phys. Rev. B **65**, 235430 (2002).
[38] M. Yoon *et al.*, Phys. Rev. Lett. **92**, 075504 (2004).
[39] D. G. Pettifor and I. I. Oleinik, Phys. Rev. B **59**, 8487 (1999).

[40] D. G. Pettifor and I. I. Oleinik, Phys. Rev. Lett. **84**, 4124 (2000).
[41] L. A. Girifalco, M. Hodak, and R. S. Lee, Phys. Rev. B **62**, 13104 (2000).
[42] T. Zhu, J. Li, X. Lin, and S. Yip, J. Mech. Phys. Solids **53**, 1597 (2005).
[43] J. Li, MRS Bull. **32**, 151 (2007).
[44] J. Rajagopalan, J. H. Han, and M. T. A. Saif, Science **315**, 1831 (2007).
[45] M. Lazzeri, S. Piscanec, F. Mauri, A. C. Ferrari, and J. Robertson, Phys. Rev. Lett. **95**, 236802 (2005).